2023 IEEE 26th International Conference on
Intelligent Transportation Systems (ITSC)
24-28 September 2023. Bilbao, Bizkaia, Spain

Spatial Change Detection Using Automotive Radar

Harihara Bharathy Swaminathan[1], Aron Sommer[2], Andreas Becker[3] and Martin Atzmueller[1,4]

***Abstract*— Detection of spatial change is indispensable in applications such as autonomous driving. In this paper, we present a method to detect spatial changes from a previously known sensor map of an environment using a suite of radar sensors mounted on a vehicle. In particular, this paper proposes a technique to detect a change in the position of a semi-static pole from the last measurement. We focus on feature construction as well as a supervised learning, trained using the respective features which describe the statistical similarity between the known map (M) and current radar sensor scan (S) of the same environment. In our experiments, we assessed different classification methods and feature configurations. Here, the support vector machine (SVM) trained using a combination of six statistical similarity features outperformed its competitors in classifying the change in position of a semi-static pole from the previously known sensor map (M) with an F1 score of 0.87.**

I. INTRODUCTION

Human error has been so far one of the common cause of road accidents. According to statistics from the German Federal Statistical Office, 88.2% of accidents resulting in personal injury in Germany were caused due to driver error [1]. In the near future, autonomous vehicles are believed to minimize road accidents by ensuring increased road safety. An autonomous vehicle is equipped with perception sensors such as lidar, camera and radar to sense the environment around it. Along with perception sensors, maps are considered to play a vital role in estimating the precise location of vehicle [2], path planning and navigation [3] when used in combination with the sensor suite of the vehicle.

Spatial change detection is concerned with finding differences and similarities between two or more pieces of geometrical information. Since it has been established that maps are an integral component along with perception sensors, the task of maintaining maps by finding outdated map-region is indispensable in the field of autonomous driving.

In this paper, we propose a spatial change detection technique, particularly for detecting a small displacement in the movement of a pole, by comparing a previously known map (M) and the current scan (S) of an environment. The spatial representations M and S are derived from 2D radar sensor measurements involving four radars mounted to the corners of a test vehicle. As an important assumption, the vehicle is considered to precisely localize itself with an accuracy of up to a few centimeters for all the experiments presented in this paper. The assumption holds true particularly for a task of map validation which is performed after position estimation of the vehicle.

Our main contributions are summarized as follows:

1) Feature construction: Spatial representations M and S are converted from point clouds to a grid based representation. The grid consists of equally spaced cells representing the space around a vehicle, where each cell in the grid could contain a probability distribution [4] modeled to represent the spread of radar detection present within it. Due to the absence of semantic knowledge of the environment, statistical features to express the similarity between probability distributions present within a cell (C) in M and S are then derived.
2) Evaluation: We compare different machine learning methods. Here, a support vector machine (SVM) trained on features derived from comparing the probability distributions within a cell (C) in map M and scan S is found to be effective (F1 score of 0.87) in detecting small displacements of a pole such as $0.5\,\mathrm{m}$, $1\,\mathrm{m}$ within the cell.
3) Robustness: As spatial change detection techniques require precise localization of the vehicle, the technique proposed in this paper was found to be robust in classifying changes correctly from non-changes, when the root mean squared (RMS) error values reported by the DGPS system was less than $10\,\mathrm{cm}$.

The rest of the paper is structured as follows: Section II discusses related work. After that, Section III presents our proposed method. Next, Section IV discusses our experimental results in detail. Finally, Section V concludes with a summary and interesting directions for future research.

II. RELATED WORK

The task of change detection has been extensively studied before for applications such as robotic surveillance and security systems for indoor and outdoor environments, [5], [6], detecting changes in an automotive high definition digital map used for automated driving [7], [8]. Andreasson, Magnusson and Lilienthal [5] proposed an autonomous change detection for a security patrol robot. For this approach, the reference map was created from multi color and depth images. Consecutively, color and depth information from 3D laser scanner and a camera were used to detect changes in spatial data. In contrast to the aforementioned sensors,

* This work was supported by Aptiv Services Deutschland GmbH

[1] Harihara Bharathy Swaminathan and Martin Atzmueller are with the Semantic Information Systems Group, Institute of Computer Science, Osnabrück University, 49069 Osnabrück, Germany. {hswaminathan, martin.atzmueller}@uni-osnabrueck.de

[4] In addition, Martin Atzmueller is also affiliated with the German Research Center for Artificial Intelligence (DFKI), Hamburger Straße 24 49084 Osnabrück, Germany

[2] Aron Sommer is with Aptiv Services Deutschland GmbH, 42119 Wuppertal, Germany aron.sommer@aptiv.com

[3] Andreas Becker is with the Faculty of Information Technology, Fachhochschule Dortmund, 44139 Dortmund, Germany andreas.becker@fh-dortmund.de

2023 IEEE 26th International Conference on Intelligent Transportation Systems (ITSC) | 979-8-3503-9946-2/23/$31.00 ©2023 IEEE | DOI: 10.1109/ITSC57777.2023.10422608

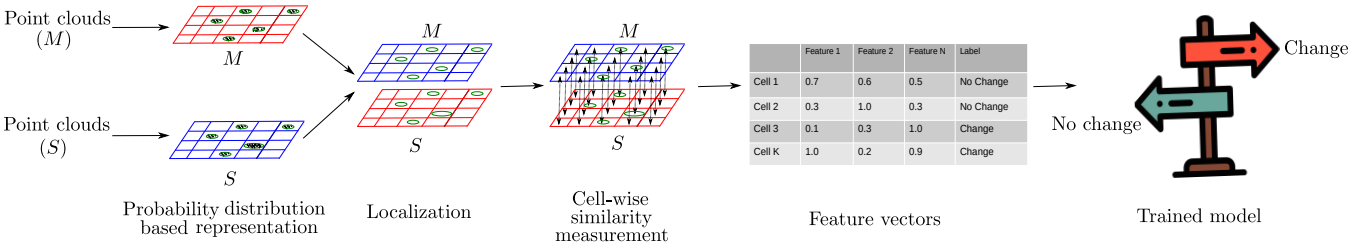

Fig. 1: An overview of the proposed spatial change detection technique.

the radar sensors does not provide color information. Palma, Cignoni, Boubekeur and Scopigno [6] proposed an approach to automatically detect geometric changes between point clouds involving a comparison of the distance to nearest points or meshes between two point clouds. However, the problem with this technique is the degree to which a proper threshold is determined. Pannen, Liebner and Burgard [7] presented a real time change detection algorithm to process data collected by series-production vehicles to detect changes in an automotive high definition digital map used for automated driving. As sensor data in [7], point landmarks such as traffic signs, poles and lane markings were used. Consequently, various metrics were computed for how well the current sensor readings match the world model in the HD map. Later, a solution for providing an up-to-date HD map with focus specifically on lane markings and road edges was presented by Pannen, Liebner, Hempel and Burgard [8]. We consider to investigate the effectiveness of automotive radar sensors in particular for the task of spatial change detection. Unlike camera and laser sensors, the task of extracting landmarks such as a pole or a traffic sign continues to be a challenge with automotive radar sensors. As a result, we aim to tackle the task of change detection using a statistical approach i.e., not involving object detectors for landmark extraction.

Overall, to the best of the authors' knowledge, a change detection technique based on statistical similarity comparison between a known sensor map and current scan of a particular environment using four corner automotive radar sensors has not yet been proposed in literature before.

III. Method

An overview of the proposed spatial change detection technique is shown in Fig 1. As part of pre-processing, the point clouds belonging to the known map (M) and the current radar scan (S) are converted to a probability distribution based representation as described in Section III-A. For the purpose of precisely aligning M and S, a high precision DGPS measurement obtained from an Applanix POS LV-220 positioning system is used. As a result of the precise alignment, a correspondence between cells in M and S can be established. During the feature extraction phase, the statistical features depicting similarity are measured by comparing cells in the probability distribution based representation of M and S as described in Section III-B. Each row of the feature table consists of similarity information derived by comparing a cell in M and its corresponding cell in S. A label such as *Change* or *No-Change* is assigned for each row of the feature vector, where the front and rear camera of the vehicle were used for verifying that objects in a particular cell did not change positions from the known map (M). At last, a supervised model is trained with the feature vectors. As a result of this data-driven approach, the supervised model is able to predict if a cell in current scan (S) has a change or not from the known map (M).

A. Probability distribution based representation

This section describes the probability distribution based spatial representation of a scan containing radar detections from the four corner radars fitted to a test-vehicle. All the radar detections have their coordinate values in the Universal Transverse Mercator (UTM) [9] system, an instance of the World coordinate system. According to the UTM system, every point on the surface of earth can be represented using an Easting, Northing coordinate, a zone number represented by an integer and an alphabet. In this work, radar detections around the vehicle are modeled with a number of local normal distributions. First, the 2D spatial region around the vehicle is subdivided regularly into cells with constant size. For each cell k with at least three points, the following steps are carried out:

1) Find all the points M_k contained in this cell depending upon the easting and northing coordinates of the cell
2) Calculate the 2×1 mean vector as in (1)

$$\mathbf{p}_k = \frac{1}{M_k} \sum_{i=1}^{M_k} \mathbf{x}_k^{(i)} = \begin{pmatrix} \mu_\mathrm{e} \\ \mu_\mathrm{n} \end{pmatrix}. \tag{1}$$

The entries represent the mean easting and mean northing coordinates of all M_k points contained in cell k.

3) Calculate the 2×2 covariance matrix as in (2)

$$\begin{aligned} \mathbf{\Sigma}_k &= \frac{1}{M_k - 1} \sum_{i=1}^{M_k} \left(\mathbf{x}_k^{(i)} - \mathbf{p}_k \right) \left(\mathbf{x}_k^{(i)} - \mathbf{p}_k \right)^\mathrm{T} \\ &= \begin{pmatrix} \sigma_\mathrm{e}^2 & \sigma_\mathrm{e}\sigma_\mathrm{n} \\ \sigma_\mathrm{n}\sigma_\mathrm{e} & \sigma_\mathrm{n}^2 \end{pmatrix} \end{aligned} \tag{2}$$

The main diagonal entries denote the variance, a measure of how far the easting and northing coordinates of all the points M_k spread out from their corresponding mean, while the anti diagonal elements denotes the covariance, a measure of how easting and northing coordinates of all the points M_k contained in the cell k

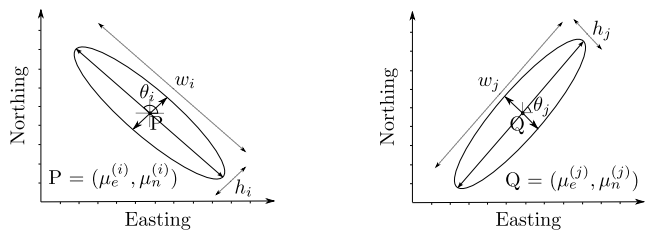

(a) Confidence ellipse from known map (M)

(b) Confidence ellipse from current scan (S)

Fig. 2: The Confidence ellipses representing normal distributions from a cell i on the known map (M) and correspondingly aligned cell j on the current scan (S).

vary together. As any covariance matrix, the matrix $\mathbf{\Sigma}_k$ is symmetric and positive semi-definite [10].

4) Calculate the probability of measuring a sample at 2D point x contained in this cell using (3)

$$p\left(\mathbf{x}\right) \sim \exp\big(-\tfrac{1}{2}\left(\mathbf{x}-\mathbf{p}_k\right)^{\mathrm{T}}\mathbf{\Sigma}_k^{-1}\left(\mathbf{x}-\mathbf{p}_k\right)\big). \quad (3)$$

B. Similarity metrics derived for classification

In the last section, the technique for modeling radar detections around the vehicle using multiple local normal distributions was introduced. In this section, a 95% confidence ellipse for a normal distribution is explained at first. Later, the statistical features for representing the similarity between previously known map (M) and the current scan (S) of an environment is explained. According to the statistical rule for a normal distribution, 95% of all values lie within two standard deviations of the mean. Due to this reason, a 95% confidence ellipse [11] drawn using the eigenvalues and vectors of the covariance matrix is used to represent the scatter of points in a cell. The eigenvalues obtained for the covariance matrix are expressed as λ_1 and λ_2, where the largest eigenvalue is defined as λ_1. The width (w) of a 95% confidence ellipse is calculated using (4) and the corresponding height (h) of the ellipse is calculated using (5) where 5.991 represents scaling factor for the 95% confidence ellipse drawn from a table of Chi-Square probabilities. In order to obtain the orientation of ellipse in degrees as seen in (6), the angle made by the largest eigenvector towards the x-axis is considered. Here $\mathbf{v_1}$ is the eigenvector of the covariance matrix corresponding to the largest eigenvalue λ_1. From now, the terms width and height of an ellipse are referred correspondingly as major and minor axis distances.

$$w = 2\sqrt{5.991\lambda_1} \quad (4)$$

$$h = 2\sqrt{5.991\lambda_2} \quad (5)$$

$$\theta = \arctan\left(\frac{\mathbf{v_1}(y)}{\mathbf{v_1}(x)}\right) \times \frac{180}{\pi} \quad (6)$$

The statistical features depicting similarity between cells in M and S are described. Furthermore, Fig 2 can be referred to obtain an understanding of the statistical features described here.

- **Difference in Mean Easting**: The difference between mean easting for a normal distribution from a cell i on the known map (M) and the correspondingly aligned cell j on the current scan (S) as expressed by (7).

$$\mathbf{\Delta}_{\mathrm{e}}^{(i,j)} = \mu_{\mathrm{e}}^{(i)} - \mu_{\mathrm{e}}^{(j)} \quad (7)$$

- **Difference in Mean Northing**: The difference between mean northing values for a normal distribution from a cell i on the known map (M) and the correspondingly aligned cell j on the current scan (S) as expressed by (8).

$$\mathbf{\Delta}_{\mathrm{n}}^{(i,j)} = \mu_{\mathrm{n}}^{(i)} - \mu_{\mathrm{n}}^{(j)} \quad (8)$$

- **Confidence ellipse major axis distance difference**: The difference between the major axis distances of a confidence ellipse from a cell i on the known map (M) and the confidence ellipse from correspondingly aligned cell j on the current scan (S) as expressed by (9).

$$\mathbf{\Delta}w^{(i,j)} = w^{(i)} - w^{(j)} \quad (9)$$

- **Confidence ellipse minor axis distance difference**: The difference between the minor axis distances of a confidence ellipse from a cell i on the known map (M) and the confidence ellipse from correspondingly aligned cell j on the current scan (S) as expressed by (10).

$$\mathbf{\Delta}h^{(i,j)} = h^{(i)} - h^{(j)} \quad (10)$$

- **Orientation in degrees difference**: The difference between orientation values of a confidence ellipse from a cell i on the known map (M) and the confidence ellipse from correspondingly aligned cell j on the current scan (S) as expressed using (11). It is represented with degrees.

$$\mathbf{\Delta}\theta^{(i,j)} = \theta^{(i)} - \theta^{(j)} \quad (11)$$

- **KL Divergence values**: The Kullback-Leibler Divergence [15] is a measure of the statistical distance between a probability distribution p from a cell i on the known map (M) and a probability distribution q from the correspondingly aligned cell j on the current scan (S). The KL divergence between the two bivariate probability distributions is expressed in (12) where Σ_q and Σ_p denote the covariance matrices, μ_q and μ_p denote the mean vectors of distributions q and p respectively and 2 represents the number of variables. If the two bivariate probability distributions are same i.e. $\mu_p = \mu_q$ and $\Sigma_p = \Sigma_q$, the KL divergence between the two distributions is zero. In addition, the KL divergence between two dissimilar distributions has a higher value than two similar distributions.

$$D_{KL}(p \parallel q) = \frac{1}{2}[\log\frac{|\Sigma_q|}{|\Sigma_p|} - 2 + (\mu_p - \mu_q)^{\mathrm{T}} \Sigma_q^{-1}(\mu_p - \mu_q) + tr\left\{\Sigma_q^{-1}\Sigma_p\right\}] \quad (12)$$

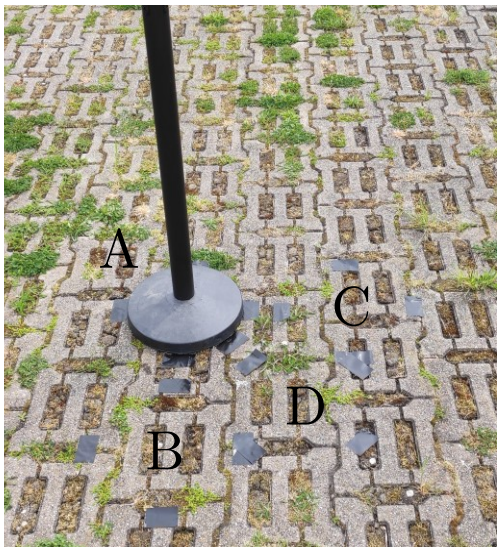

(a) The semi-static pole

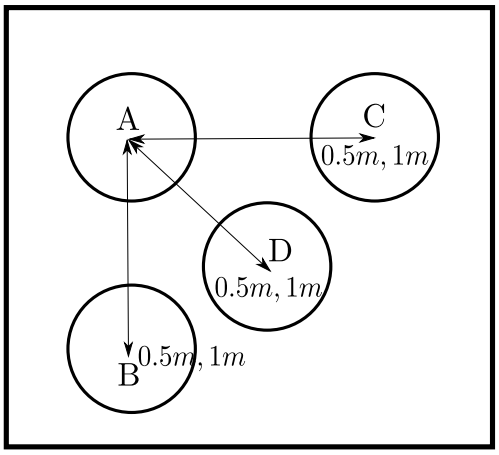

(b) Displacement of the pole in a cell

Fig. 3: The Semi-static pole and its corresponding displacement positions for the experiments at a parking lot. Here, A denotes original position of the pole, C denotes lateral displacement to the right of original position, D denotes diagonal displacement , B denotes Longitudinal displacement. Furthermore, the pole was moved at $0.5\,\mathrm{m}$ and $1\,\mathrm{m}$ distances from A.

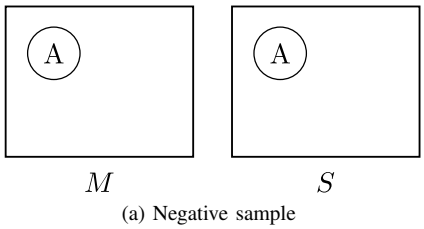

(a) Negative sample

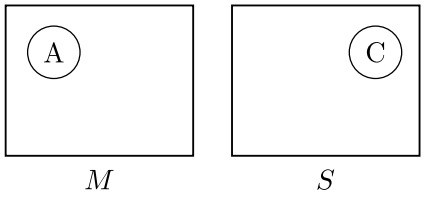

(b) Positive sample

Fig. 4: Instances of a negative and positive sample in the change detection dataset.

IV. Experimental Results

In this section, a series of experiments are presented. The objective is to verify if the proposed approach is capable of detecting even a small change in the position of a pole. The test-vehicle used for the experiments was equipped with an Applanix POS LV-220 high precision positioning system capable of receiving Trimble CenterPoint RTX GNSS corrections [12], onboard perception sensors such as radars fitted to the corners, camera facing the front and rear of the vehicle and lidar sensor. The semi-static pole and its displacement for the experiments are shown in Fig. 3a and Fig. 3b respectively. For the purpose of introducing a change to the original position (A) of the pole, it was moved in three-different variations such as lateral (C), longitudinal (B) and diagonal (D) at $0.5\,\mathrm{m}$ and $1\,\mathrm{m}$ distances from the original position (A) in between the laps. Additionally, multiple laps were driven with the pole remaining at its original position (A). On every lap, the vehicle was driven at a set distance and speed adjacent to the pole. Also, it was ensured that the pole was not hidden away at any point during the course of a lap from all the radars. During the course of every lap, the position error values obtained from the Applanix POS LV-220 system were monitored to ensure that they do not rise and during the data-analysis, all the laps with rms error values more than $10\,\mathrm{cm}$ were discarded from the dataset preparation.

For training a supervised model, *Change* and *No-Change* data samples are created using a combination of known map (M) and current sensor scan (S). An instance of a No-change sample is created by comparing two laps with no displacement in the pole's position between the laps. For e.g., both the known map (M) and the current sensor scan (S) are created with the pole at its original position as shown in Fig. 4a. On the other hand, an instance of a Change sample is created by comparing two laps with a pole displaced between the laps. For e.g., the known map (M) is created from the lap with the pole at its original position and current sensor scan (S) is created with the pole at $1\,\mathrm{cm}$ lateral displacement as shown in Fig. 4b. A row of the change detection dataset consists of handcrafted features derived using various lap combinations for Map (M) and Current scan (S) and a label which is denoted with 0 (No-Change) or 1 (Change). All the statistical features derived from the known map (M) and current sensor scan (S) comparisons are described in the previous section. The complete dataset comprised of 22.2% positive samples and 77.8% negative samples. For labeling, a visual approach was followed using the front and rear camera of the vehicle for verifying that objects in the remaining cells remain stationary. For the sake of convenience, the

		Truth		
		Change	No-change	Total
Predictions	Change	a	b	$a+b$
	No-change	c	d	$c+d$
	Total	$a+c$	$b+d$	N

TABLE I: Elements of a confusion matrix for the change detection problem.

experiments were carried out at a parking lot at a time when there are less movement of vehicles.

For finding the best classifier, a k-nearest-neighbors (kNN) classifier with $k = 7$, a random forest classifier (RFC) and a support vector machine (SVM) with a Radial Basis Function (RBF) kernel [13] were trained. In order to estimate the efficiency of the model on unseen data, a 5-fold cross validation approach [14] was applied which is effective for finding the skill of a classifier using limited data samples and reduces overfitting to a training dataset. In this approach, the entire dataset is divided into 5 subsets/folds and the model is trained and evaluated 5 times, using a different data subset each time. At the end, the performance metrics from each fold are averaged to estimate the model's generalization performance. Since, Accuracy can be a misleading performance metric for imbalanced datasets, we make use of Precision, Recall and F1 scores for evaluating the predictions of the applied classifiers. Table I shows the elements of confusion matrix for the change detection problem for calculating the Precision and Recall scores.

Precision is defined as the number of true positives over the number of true positives plus the number of false positives as expressed by (13).

$$P = \frac{a}{a+b} \tag{13}$$

Recall is defined as the number of true positives over the number of true positives plus the number of false negatives as expressed by (14).

$$R = \frac{a}{a+c} \tag{14}$$

The F1 score is defined as the harmonic mean of precision and recall as expressed by (15).

$$F1 = 2 \cdot \frac{P \cdot R}{P+R} \tag{15}$$

All the aforementioned scores range from 0 to 1. For the sake of intuition, it can be said that a sub-optimal precision score indicates a high number of false positives and a sub-optimal recall score indicates a high number of false negatives. A good classifier is characterized by precision, recall and F1 score close to 1. Since the number of positive samples are less in the dataset, we give importance to recall scores over precision scores.

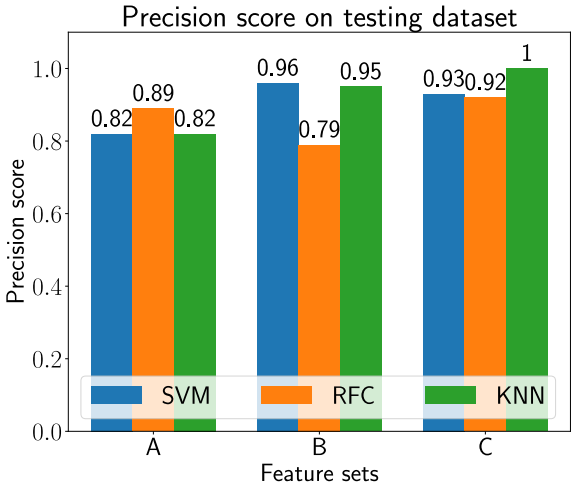

(a) Precision

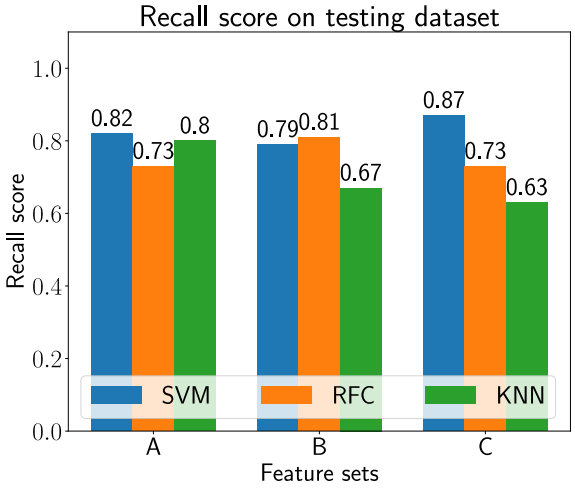

(b) Recall

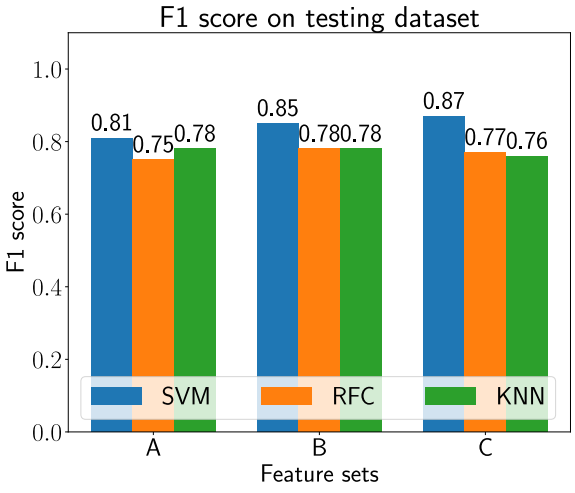

(c) F1-score

Fig. 5: Average Precision, Recall and F1 scores (5-fold cross validation) for the classifiers K-Nearest Neighbour (KNN), Random Forest Classifier (RFC) and a Support Vector Machine (SVM) trained on feature sets A, B and C.

The average of the Precision, Recall and F1 scores obtained during a 5-fold cross validation process for various

classifiers such as the KNN, RFC and SVM trained using feature sets A, B and C are shown in Fig. 5a, Fig. 5b and Fig. 5c respectively. In each of these figures, the letter 'A' is used to denote the combination of 2 features i.e. difference in mean easting and difference in mean northing, the letter 'B' is used to denote the combination of 5 features i.e. confidence ellipse major axis distance difference, confidence ellipse minor axis distance difference and orientation difference in degrees along with the features represented by letter 'A'. Finally , the letter 'C' is used to denote the combination of 6 features including KL-Divergence along with those represented by 'A' and 'B'. According to Fig. 5b and Fig. 5c, the best classification was obtained using an SVM trained with a combination of all the six statistical features denoted by 'C' with an average recall and F1-score of 0.87 over the testing dataset. In addition, the feature set represented by letter 'A' i.e. difference in mean easting and difference in mean northing is predominant for the classification because of good recall and F1 scores (> 0.7) for the classifiers trained during these experiments. A significant improvement in the F1-score (from 0.81 to 0.87) and recall score (from 0.82 to 0.87) of the SVM, as observed in Fig. 5b and Fig. 5c can be attributed to the inclusion of Kullback-Leibler divergence values (denoted using letter 'C') as part of feature set.

V. Conclusions

In this paper, we presented an approach for the detection of spatial changes from a previously known map (M) with respect to an environment using automotive radar sensor data. As a target object, a semi-static pole was placed on a parking lot. The main objective of the experiments is to verify if the proposed approach is effective in detecting a small displacement of the pole from its original position. As part of the presented approach, a set of simple statistical features were derived from comparing the previously known map (M) and current scan (S) of the same environment. For the purpose of a precise localization, a high precision, high cost DGPS system was used. One of the vital intermediate step involves a probability distribution based representation of the map (M) and sensor scan (S) for deriving statistical features. The best results were obtained from training a support vector machine (SVM) classifier using a combination of six statistical features described in this work, with an average F1 score of 87% on the test dataset. Other crucial inferences from experiments involved the identification of similarity measurement features such as Kullback-Leibler Divergence with a positive impact on model performance.

For future work, the ability of the proposed approach for detecting changes such as appearance of a construction zone, addition or removal of a static object such as a traffic sign should be investigated on a more challenging environment than the parking lot. In addition, further research should be carried out to find approaches where the similarities/differences between the previously known map (M) and current scan (S) of the same environment could be self-learned directly from the input data.

References

[1] W. Sigloch, High Risk of Accidents caused by People's behaviour, Press release of Dekra e.V., Stuttgart, Germany, August 2021.

[2] A. Pishehvari and U. Iurgel and M.Stefer and B. Tibken, Range-Doppler Registration, Proc. IEEE International Conference on Control and Robotics Engineering (ICCRE'20), Osaka, Japan, April 2020, pp. 169-176

[3] A. Diaz-Diaz and M. Ocaña and Á. Llamazares and Gómez-Huélamo, HD maps: Exploiting OpenDRIVE potential for Path Planning and Map Monitoring, Proc. IEEE Intelligent Vehicles Symposium (IV'22), Aachen, Germany, June 2022, pp. 1211-1217

[4] P. Biber and W. Straßer, The normal distributions transform: A new approach to laser scan matching, Proc. IEEE/RSJ International Conference on Intelligent Robots and Systems (IROS 2003), Las Vegas, NV, USA, Oct 2003, pp. 2743-2748

[5] H. Andreasson and M. Magnusson and A. Lilienthal, Has something changed here? Autonomous difference detection for security patrol robots, Proc. IEEE/RSJ International Conference on Intelligent Robots and Systems (IROS 2007), San Diego, CA, USA, Oct 2007, pp. 3429-3435

[6] G. Palma and P. Cignoni and T. Boubekeur and R. Scopigno, Detection of geometric temporal changes in point clouds, Computer Graphics Forum, Wiley Online Library, Oct 2015, pp. 33-45

[7] D. Pannen and M. Liebner and W. Burgard, HD Map Change Detection with a Boosted Particle Filter, Proc. IEEE International Conference on Robots and Automation (ICRA 2019), Montreal, QC, Canada, May 2019, pp. 2561-2567

[8] D. Pannen and M. Liebner and W. Hempel and W. Burgard, How to keep HD maps for automated driving up to date, Proc. IEEE International Conference on Robots and Automation (ICRA 2020), Paris, France, May 2020, pp. 2288-2294

[9] L.M.Bugayevskiy and J. Snyder, Map projections: A reference manual, CRC Press, 1995, pp. 163

[10] R.A. Hohnson and D.W.Wichern, Applied multivariate statistical analysis, 2007, Prentice Hall

[11] O. Erten and C.V. Deutsch, Combination of multivariate Gaussian distributions through error ellipses, Geostatistics lessons, 2020

[12] H.B. Swaminathan and A. Sommer and A. Becker and M.Atzmueller, Performance Evaluation of GNSS Position Augmentation Methods for Autonomous Vehicles in Urban Environments, Sensors, vol. 22, Nov 2022, pp. 8419

[13] F. Pedregosa and G. Varoquaux and A. Gramfort and V. Michel, Scikit-learn: Machine Learning in Python, Journal of Machine Learning Research, vol. 12, 2011, pp. 2825-2830

[14] R. Kohavi, A study of cross-validation and bootstrap for accuracy estimation and model selection, Proc. International joint Conference on artificial intelligence, vol. 14, 1995, pp. 1137-1145

[15] S. Kullback and R.A. Leibler, On information and sufficiency, The Annals of Mathematical Statistics, vol. 22, 1951, pp. 79-86